Technical University of Denmark

DTU

A Fast Forward Electromagnetic Solver for Microwave Imaging

Chaber, Bartosz; Mohr, Johan Jacob

DTU Library
Technical Information Center of Denmark

Bartosz CHABER[1], Johan Jacob MOHR[2]

Warsaw University of Technology (1), Technical University of Denmark (2)

A fast forward electromagnetic solver for microwave imaging

Abstract. This paper describes an efficient model of an antenna system for microwave imaging. The authors present techniques employed in the process of preparation of this model, as well as an accuracy comparison with the working prototype system.

Keywords: microwave imaging, nonlinear inverse problems, radio frequency, computational methods, meshing, breast cancer

Background

Microwave imaging is a technique that allows for noninvasive tomography with the use of transmitting antennas. It is based on measurements of a scattered field. The scattered field is generated due to an inhomogeneous distribution of electrical parameters in the region between the antennas. An illustration of the effect of a scatterer is presented in Fig. 1.
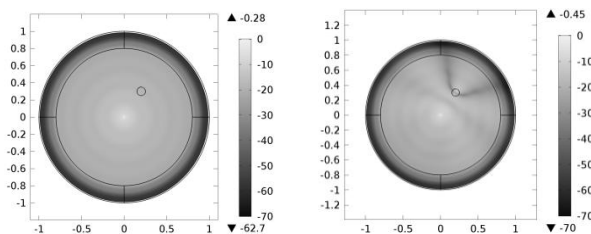

Fig.1. Magnitude of an electric field (in dB with respect to the maximum value) from a current source (its direction is normal to the plane; frequency is 800 MHz) in two cases: without scatterer (left) and with a scatterer (right). The scatterer has the radius of 5 cm and $\varepsilon_r = 6$). The domain in both cases is air ($\varepsilon_r = 1$).

During data acquisition, one antenna acts as transmitter while the rest are receiving. The process is repeated for each antenna as a transmitter and as the result we get off-diagonal elements of the scattering matrix. Based on the measurements one can solve a nonlinear inverse scattering problem [1] and obtain an approximation of an unknown distribution of the contrast function χ in the region surrounded by the antennas (the region is known as the imaging domain). The unknown contrast function describes the electrical permittivity and conductivity distributions. In this paper, we present the technique in the context of breast cancer detection where a malignant tissue are embedded in an in-homogenous background acts as a scatterer.

In order to solve the nonlinear inverse problem often a linearization method is employed (e.g. distorted wave Born approximation) followed by a linear optimization solver. The forward electromagnetic solver is then used to evaluate the "guess" of the unknown distribution and calculate scattering parameters (S-parameters) together with electric field values in the imaging domain. The electric field values can be used to assess correctness of the process.

The need of a fast electromagnetic field solver

In this paper the linear optimization solver requires at least 20 iterations to obtain a good image. It puts some time restrictions on the full field solver. In a prototype context, the whole process should take not more than 12 hours.

Right now, an in-house Method of Moments solver [2] is used as the forward electromagnetic field solver. It is fast, accurate and tested. However it has some limitations which pushed authors' focus towards commercial software. The

most significant disadvantages of the solver are: a steep learning curve, the tedious process of building a model and lack of portability. Most of commercial software packages provide users with advanced tools for model building and meshing. It is especially important in development phase, when rapid building an efficient digital prototype is crucial. Commercial software tends to be more general and have better post-processing capabilities which make model inspection easier and faster. The portability and documentation is often far better than in an in-house software. This leads to much easier knowledge transfer. All those features enable the authors to pursue better imaging system. After the prototype is improved and not going to be further modified, one can substitute the full field solver with the former, dedicated one, to take advantage of its speed.

Prototype system

The current prototype system (described in more details in [3]) consists of a large tank filled with a coupling liquid. Inside the tank there are 8 layers of 4 monopole antennas (see Fig. 2). Each of the antennas is made out of a coaxial cable with 3.5 cm of the outer conductor stripped. The antennas are placed in a circular layout with the imaging domain in their center. The imaging domain has the radius of 7.5 cm and the height of 12 cm. The system is operating in the frequency range from 0.5 to 2 GHz. The coupling liquid is a 90-10% glycerol-water solution. The electrical parameters of the liquid that have been measured with a dielectric probe kit are: $\varepsilon_r = 9.45$ and $\sigma = 0.843$ S/m at 1.5 GHz at 22 °C. From this it follows that the wavelength in the liquid is about 6 cm.

Fig.2. Top view of the tank with antennas and their data acquisition units.

The advanced switching and acquisition system controlling the device is not the part of the presented numerical simulation. For further information about the system see [3].

Numerical model

A computer model of the prototype presented in the previous section was prepared. As a result of using a lossy coupling liquid the model assumed that there is no reflection from the walls of the tank. The model assumed also that the exterior radiation is attenuated and does not influence the antennas readings. This was enforced using a cylindrical Perfectly Matched Layer on boundaries of the domain.

To simplify the model the wave equation is solved only in the liquid, imaging domain and the antennas dielectrics. Due to the skin effect we discretize only surfaces of the unstripped parts of the antennas.

There has been a great deal of attention paid to meshing the model. A special care had to be taken of mesh inside of the imaging domain. To avoid instabilities in the inverse solver part of the imaging algorithm, due to interpolation errors in the COMSOL field solution, we use a fixed mesh in the imaging domain. In order to simplify interfaces between different processing and visualization elements of the entire image formation chain, a regular hexahedral mesh is preferable. Unfortunately, a tetrahedral mesh is much more desirable in the remaining part of the COMSOL model due to its flexibility, but a regular hexahedral mesh cannot be sub-divided into a regular tetrahedral mesh. Therefore, a hybrid method has been chosen, where the outer layer of the imaging domain mesh is discretized using prism elements connecting the hexahedral and tetrahedral meshes. Different layers of the mesh can be seen in Fig. 3. For the illustration of the process of meshing the imaging domain see Fig. 4.
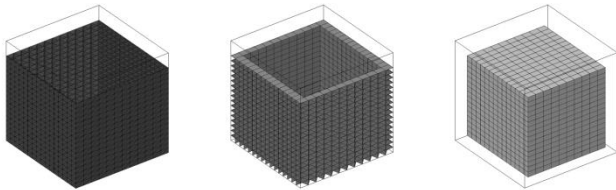

Fig.3. Three types of mesh elements in the imaging domain. From left: tetrahedra, prisms and hexahedra.
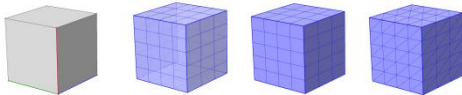

Fig.4. Process of meshing the imaging domain. From left: no mesh, a mapped mesh on the boundary, swept interior of the imaging domain, the boundary elements converted to triangles.

After the preparation of the initial model, the elements of the worst quality had been plotted. They appeared at the interfaces between dielectrics and outer conductors. Making the mesh denser at the interfaces increased the overall mesh quality, which in turn improved the convergence of the solution when using an iterative solver.

The material parameters of the liquid vary with frequency, temperature and the ratio between glycerol and water. It was reflected in the numerical model using Cole-Cole approximation for the given temperature and ratio. For the 90-10% solution at 24 °C the following Cole-Cole parameters were used: ε_s = 45.6, ε_∞ = 4.78, τ = 400 ps, α = 0.106, σ_s = 0.019 S/m. The parameters were obtained by fitting to the measurements of the parameters taken with an Agilent 85070 E dielectric probe kit. The results of the approximation are depicted in Fig. 5. As one can see in the plot, the electrical parameters ε' and ε'' are better fitted for frequencies higher than 1.1 GHz.
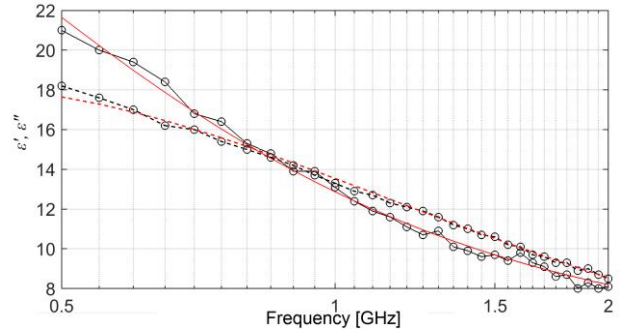

Fig.5. Cole-Cole model of the 90-10% glycerol-water solution at 24 °C used in the simulation.

Communication between COMSOL and inverse solver

There are different ways of connecting COMSOL simulations with the rest of a processing toolchain. One is to use the MATLAB LiveLink connection to define the model with MATLAB scripts. In this paper a simpler (file-based) approach is presented. Using a simple text file in the COMSOL grid format one can import the contrast function χ. A sample input file is presented below:

```
% grid
-0.04 -0.02 0.00 +0.02 +0.04
-0.04 -0.02 0.00 +0.02 +0.04
-0.04 -0.02 0.00 +0.02 +0.04

% data
1 1 1 1 1   1 1 1 1 1   1 1 1 1 1   1 1 1 1 1   1 1 1 1 1
1 1 1 1 1   1 2 2 2 1   1 2 2 2 1   1 2 2 2 1   1 1 1 1 1
1 1 1 1 1   1 2 2 2 1   1 1 3 1 1   1 2 2 2 1   1 1 1 1 1
1 1 1 1 1   1 1 2 1 1   1 2 1 2 1   1 1 2 1 1   1 1 1 1 1
1 1 1 1 1   1 1 1 1 1   1 1 1 1 1   1 1 1 1 1   1 1 1 1 1
```

This contrast function distribution is visualized in Fig. 6 (each line in data section is a slice). The function was imported as **chi**, using nearest neighbor interpolation and constant value extrapolation. It was used as the scaling factor of electrical permittivity in the material properties of the liquid: **liquid_epsr * chi(x, y, z)**.
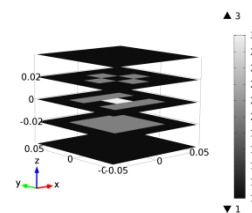

Fig.6. A contrast function imported from a COMSOL grid file as an interpolating function (using nearest neighbor interpolation).

Choosing the most efficient solving method

One of the advantages of using a commercial package for building a full field solver is the ease of switching between different linear solvers. In the case of the electromagnetic solver presented in this paper, the biggest improvement in terms of speed was made by switching from GMRES iterative solver to a direct solver (i.e. PARDISO). This change decreased the calculation time over 2 times (226%) while increasing memory usage almost 2 times (174%) for the simple model (one monopole antenna). MUMPS solver can be considered as an alternative to PARDISO, however the calculation time of MUMPS was about 2 times (172%) slower than PARDISO solver for the

full model of 32 antennas. The memory usage is similar for both MUMPS and PARDISO. Due to possibly large condition number of the full problem, neither GMRES nor BiCGStab could converge to a solution.

Validation with measurements

In order to assess usefulness of the solver, its results were compared to measurements. The experiment compares the measurements of the empty tank with the corresponding numerical model. In this section the measurements are compared with simulation results. The measurements were taken with a VNA HP8753c by directly connecting its cables to the antenna ports. One of the cables had to be connected with a female to female adapter. The phase delay of the adapter had been removed during the calibration process. Six possible sources of inaccuracies are discussed. The sources are:

1. attenuation and phase delay due to difference in the placement of ports in COMSOL and VNA,
2. unsymmetrical antennas placement,
3. manufacturing imperfections of the monopoles,
4. coupling between the antennas,
5. unknown liquid parameters,
6. VNA's uncertainties.

The monopole antennas in the prototype are made of a coaxial cable and excited at the port outside of the tank, while in the COMSOL simulation an excitation is applied at the beginning of the exposed dielectric. Between the two ports (marked as VNA and COMSOL, respectively in Fig. 7) the cable attenuates a signal and introduces a phase delay.
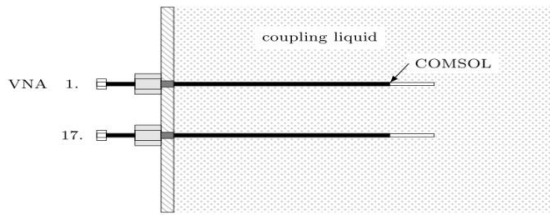

Fig.7. Side view of two antenna placements (antenna 1 and 17) with VNA and COMSOL ports marked.

The effect of the coaxial cable was calculated using data from Micro-Coax Datasheet [4] and (1).

$$(1) \qquad \Gamma_{VNA} = e^{-2\gamma l}\, \Gamma_{COMSOL},$$

where: Γ_{VNA} is the reflection measured by the VNA, Γ_{COMSOL} is the reflection calculated by COMSOL and $\gamma = \alpha + j\beta$.

The attenuation and phase delay introduced by the cable are presented in Fig. 8. All the results presented further in this paper are corrected using the relation between VNA measurements and COMSOL calculations. The transmission coefficient magnitude (in linear scale) in COMSOL is about 3-7% lower than VNA readings.

Due to an extensive usage of the system during measurements and possibly during the manufacturing process, the symmetry in the antenna positions has been broken. This helps assessing the sensitivity of the system with respect to geometric imperfections, and it should be considered in future designs of an improved microwave imaging device. The modified geometry differs from the nominal in positions of antenna 1, 3 and 5. The antennas had been displaced as follows: antenna 1 by $\Delta x = -2$ mm, $\Delta y = -1$ cm, antenna 3 by $\Delta y = -2.5$ mm and antenna 5 by $\Delta x = +2$ mm. For the purpose of verification, only the

magnitude of transmission between the antenna number 5 and 1 has been compared.
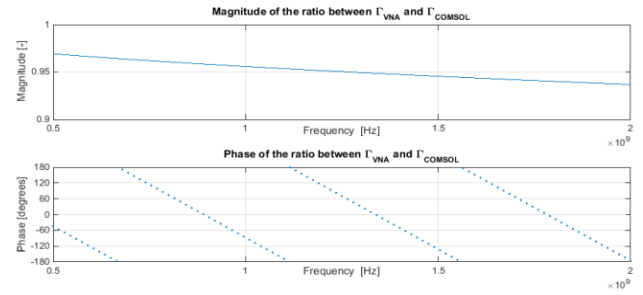

Fig.8. The relation between Γ_{VNA} and Γ_{COMSOL}.

The magnitude of S_{51} for the modified geometry is larger than the value from the simulation of the original geometry (it differs by 0.4 dB for 500 MHz and by 1.0 dB for 1 GHz). The highest difference between the measurements and the simulation of the actual geometry is about 5 dB.

After a careful inspection of the antennas it turned out that during the manufacturing process, the dielectric of the monopole is 0.5 mm shorter, exposing 0.5 mm of the inner conductor. Two additional monopole antennas have been manufactured: one without the inner conductor exposed (called *original*) and one with the exposed inner conductor tip. To confirm that the difference comes from the exposed inner conductor a 2D simulation of a single monopole antenna was prepared. It has to be noted that modeling of the exposed inner conductor makes the mesh much denser at the ends of the antenna.
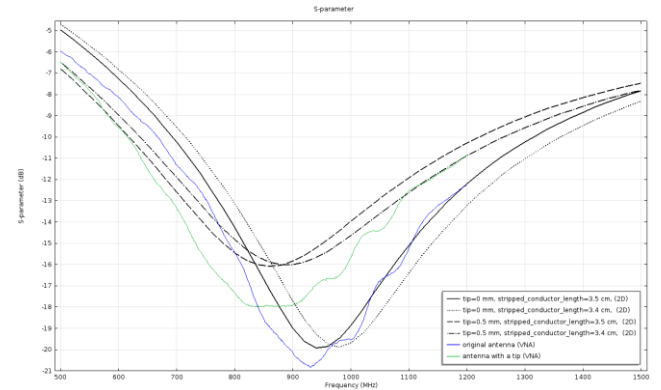

Fig.9. The effect of the exposed inner conductor confirmed by the 2D simulation of a single monopole antenna. The original monopole has its resonance frequency at around 920 MHz, while the one with the tip at around 850 MHz. The original monopole seems to have a lower reflection for its resonance frequency then the other one.

The last potential source of discrepancies that is related to geometric imperfections is the distance between the layers of antennas. In the prototype device the distance between the antennas is very small due to a slight bend of the antennas. It was confirmed during measurements that the distance between two antennas has a significant influence on S_{11} (Fig. 10). A possible explanation of this behavior is a coupling between the antennas. However, the simulation of the effect couldn't be done, because placing the layers so close to each other resulted in such a dense mesh that was impossible to solve due to RAM limitations.

Due to the lack of exact data on electrical parameters of glycerol-water solution an approximation had to be done using data from measurements with the mentioned Agilent

dielectric probe kit. This introduced two factors that may affect simulation results: parameters measurement uncertainties and approximation errors.
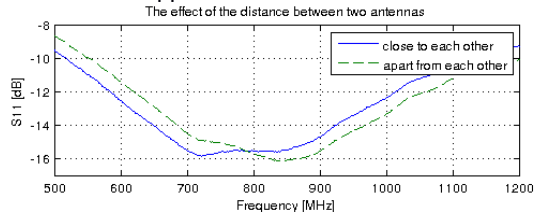

Fig.10 The effect of the exposed inner conductor confirmed by the 2D simulation of a single monopole antenna.

Originally the 90-10% glycerol-water solution was used as the coupling liquid, but results from Table 1 might suggest that over time, the ratio between glycerol and water increased (due to a water evaporation). The Cole-Cole approximation for 95-5% solution was impossible due to the lack of measurement data for this mixture.

Table 1. Comparison of results for two different liquid mixtures.

Magnitude S_{15}	500 MHz	1 GHz
85-15%	−65.7 dB	−84.7 dB
90-10%	−64.5 dB	−81.8 dB
Measurements	−60.1 dB	−81.8 dB

The last source of differences is the measurements uncertainty itself. Fig. 11 presents plots of uncertainty for each measured transmission by HP 8753D (note that the measurements presented in this paper were taken using HP 8753C, but the uncertainty between the two models was assumed to be similar). As one can see from the plots, the uncertainty for −60 dB is about ±0.2 dB and ±1° while for −80dB it is around ±1.2 dB and ±8.5°.
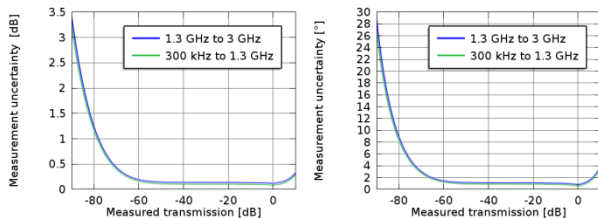

Fig.11. The plot of uncertainty in relation to the measured transmission magnitude (on the left: uncertainty in magnitude, on the right: uncertainty in phase).

Discussion of verification with measurements

In the previous section six potential sources of discrepancies were presented. Three of them have been addressed in the numerical model (1, 2 and 6) while the other three remained unsolved.

The effect of exposed inner conductor has been confirmed by a 2D simulation and applied to the full 3D model. However, it significantly increased mesh complexity, which lead to almost two times longer computational time (25 minutes instead of 15 minutes for one frequency). Modeling of the coupling between the antennas turned out to be unfeasible due to enormous RAM consumption (around 180 GB) using the PARDISO solver.

During the research an effect of liquid parameters had been assessed. A more accurate method of identification of electrical parameters of liquids would be useful for monitoring the coupling liquid in the device. For now one possible explanation is that due to a water evaporation the coupling liquid has a higher glycerol-water ratio than 90/10.

In the presented results only the magnitude was shown. In the current state of the model, the value of phase is not determined in a quantitatively way, although the relation between phases seem to be correctly calculated by the numerical model.

Due to the mesh complexity the coupling couldn't be reproduced by the numerical model. However, the effects of the exposed inner conductor and unsymmetrical antenna placement were possible to be confirmed using the simulations. This makes the full field solver also an useful tool for investigating the physical prototype by carrying out numerical experiments to see the influence of different (often unwanted) features of the microwave imaging system. It is now possible to build another physical prototype without the geometrical imperfections and with a known glycerol-water ratio of the coupling liquid. Such a device should be accurately modeled with the solver.

Conclusions

This paper shows that finite element method is a viable tool for building a fast forward solver for microwave imaging. With the help of commercial packages building a complex geometry model and inserting the solver in an existing toolchain is feasible is a reasonable time. The accuracy of the solver is acceptable and the discussion on potential sources of discrepancies has been presented in the paper. Because the imaging system is calibrated with an empty tank before the actual measurements, the reported discrepancies are not so critical for the system.

A frugal meshing scheme and a technique for communication between the solver and the rest of the imaging system have also been presented. In order to decrease the computational time authors suggest using direct solvers However, if the speed is a much more important factor than flexibility and ease of use, a more dedicated solver should be used as the electromagnetic field solver [2, 5 and 6].

REFERENCES
[1] Hansen, P. C. (2010). Discrete Inverse Problems. Fundamentals of Algorithms. SIAM - Society for Industrial and Applied Mathematics. http://doi.org/10.1086/640981
[2] Oleksiy S. Kim, Peter Meincke, Adaptive Integral Method for Higher Order Method of Moments, IEEE Transactions on Antennas and Propagation, 56 (2008), No. 8
[3] V. Zhurbenko, T. Rubæk, V. Krozer, P. Meincke, Design and realisation of a microwave three-dimensional imaging system with application to breast-cancer detection, IET Microwaves, Antennas & Propagation, 2010
[4] Micro-Coax UT-141-SS datasheet, http://www.microstock-inc.com/pdfshow01.php?item=UT-141B-SS (access: 01.06.2015)
[5] Scapaticci, R., Kosmas, P., & Member, S. (2015). Wavelet-Based Regularization for Robust Microwave Imaging in Medical Applications. *IEEE Transactions on Biomedical Engineering*, *62*(4), 1195–1202.
[6] Simonov, N., Son, S.-H., Kim, B.-R., Lee, K.-J., & Jeon, S.-I. (2014). A Fast Electromagnetic Solver for Microwave Medical Imaging. In *IEEE MTT-S International Microwave Workshop Series on RF and Wireless Technologies for Biomedical and Healthcare Applications* (*IMWS-Bio*) (pp. 1–3). London: IEEE. http://doi.org/10.1109/IMWS-BIO.2014.7032409

Authors: Bartosz Chaber, Warsaw University of Technology, Koszykowa 75, 00-662 Warsaw, Poland, chaberb@iem.pw.edu.pl Johan Mohr, Technical University of Denmark, Ørsteds Plads, 2800 Kgs. Lyngby, Denmark, jm@elektro.dtu.dk